Transcranial Measurement of Cerebral Microembolic Signals During Pulmonary Vein Isolation: A Comparison of Two Ablation Techniques

Edina Nagy-Baló, Diana Tint, Marcell Clemens, Ildikó Beke, Katalin Réka Kovács, László Csiba, István Édes and Zoltán Csanádi

Circ Arrhythm Electrophysiol. 2013;6:473-480; originally published online April 11, 2013;
doi: 10.1161/CIRCEP.112.971747
Circulation: Arrhythmia and Electrophysiology is published by the American Heart Association, 7272 Greenville Avenue, Dallas, TX 75231

Print ISSN: 1941-3149. Online ISSN: 1941-3084

Transcranial Measurement of Cerebral Microembolic Signals During Pulmonary Vein Isolation

A Comparison of Two Ablation Techniques

Edina Nagy-Baló, MD; Diana Tint, MD, PhD; Marcell Clemens, MD; Ildikó Beke, MD; Katalin Réka Kovács, MD; László Csiba, MD, PhD, DSc; István Édes, MD, PhD, DSc; Zoltán Csanádi, MD, PhD

Background—Pulmonary vein isolation has increasingly been used to cure atrial fibrillation, but concerns have recently been raised that subclinical brain damage may occur because of microembolization during these procedures. We compared the occurrence of bubble formation seen on intracardiac echocardiography and the microembolic signals (MESs) detected by transcranial Doppler on the use of different ablation techniques and anticoagulation strategies.

Methods and Results—This prospective study included 35 procedures in 34 consecutive patients (age, 52; SD, 12.8 years; female:male 9:25). Pulmonary vein isolation was performed with a cryoballoon and the conventional anticoagulation protocol (activated clotting time >250 s) in 10 procedures (group 1), with a multipolar duty-cycled radiofrequency pulmonary group 2), and with regime a pulmonary vein ablation catheter with an aggressive anticoagulation (activated clotting time >320 s) in 13 procedures (group 3). The mean total numbers of MESs detected during the procedures were 833.7 (SD, 727.4) in group 1, 3142.6 (SD, 1736.4) in group 2, and 2204.6 (SD, 1078.1) in group 3 (P=0.0005). MESs were detected mostly during energy delivery in the pulmonary vein ablation catheter groups, whereas a relatively even distribution of emboli formation was seen during cryoballoon ablations. A significant correlation was found in all groups between the degree of bubble formation on intracardiac echocardiography and the number of MESs (P=0.0000).

Conclusions—Duty-cycled radiofrequency ablation is associated with significantly more MESs, even when more aggressive anticoagulation is applied. With both techniques most of these microemboli are gaseous in nature. **(*Circ Arrhythm Electrophysiol*. 2013;6:473-480.)**

Key Words: atrial fibrillation ■ cerebral microemboli ■ pulmonary vein isolation ■ transcranial Doppler

Manifest stroke and transient ischemic attacks are among the most fearful adverse events during transcatheter ablation for atrial fibrillation (AF), with an occurrence rate of around 1%.[1] Recent data suggest, that clinically apparent cerebral ischemia is only the "tip of the iceberg" because silent ischemic lesions can be demonstrated by diffusion-weighted cerebral MRI in a much higher proportion of the patients undergoing left atrial (LA) ablation.[2–7] Although the clinical relevance of these lesions is unknown, they raise new concerns regarding the safety of AF ablation. Importantly, a significant correlation has been demonstrated between the incidence of these cerebral lesions and the ablation technology used: circular multipolar phased radiofrequency (RF) ablation has consistently been associated with the highest incidence of new lesion formation, in up to 37% of the procedures, whereas cryoenergy seems to be the safest technique.[8]

Editorial see p 455
Clinical Perspective on p 480

Real-time assessment of the thromboembolic risk during LA ablation with the potential to guide energy delivery, thereby improving procedure safety, is intriguing. To date, 2 methods have been used for this purpose: the monitoring of microbubbles on intracardiac echocardiography (ICE) and the detection of microembolic signals (MESs) in the cerebral arteries by transcranial Doppler (TCD). The titration of RF energy based on the intensity of microbubble formation during LA ablation was first proposed by Kilicaslan et al[9] and has become routine practice in many centers. Limited data are available on the number of MESs during LA ablation for AF. In a recent report, significantly more MESs were detected with the use of irrigated RF energy as compared with cryoablations,[10] confirming previous MRI findings, which suggested an ablation technology–dependent risk of nonclinical cerebral ischemia. However, currently there are no data available regarding the composition of these MESs, although multifrequency TCD has the ability to discriminate between the solid and the gaseous types. Furthermore,

Received March 4, 2012; accepted March 26, 2013.

From the Institute of Cardiology (E.N.-B., D.T., M.C., I.B., I.E., Z.C.), and Department of Neurology (K.R.K., L.C.), University of Debrecen, Debrecen, Hungary.

The online-only Data Supplement is available at http://circep.ahajournals.org/lookup/suppl/doi:10.1161/CIRCEP.112.971747/-/DC1.

Correspondence to Edina Nagy-Baló, MD, Institute of Cardiology, University of Debrecen, 22 Móricz Zs. Krt., Debrecen H-4032, Hungary. E-mail edinanagybalo@yahoo.com

the distribution of MESs during the different stages of AF ablation procedures involving different types of energy and the potential influence of different anticoagulation regimes on the number of MES have not been studied yet.

The aims of the present study were, therefore, to investigate cerebral microembolization during different stages of LA ablation with a cryoballoon (CB) versus multipolar phased RF technology and the pulmonary vein ablation catheter (PVAC), and also the ratio of solid/gaseous emboli and the influence of different anticoagulation strategies on the MES burden.

Methods

Patients

Thirty-four consecutive patients undergoing pulmonary vein isolation (PVI) for symptomatic paroxysmal or persistent AF not adequately controlled by ≥1 antiarrhythmic drug were eligible for inclusion in the study. The exclusion criteria included long-standing persistent AF, hyper- and hypothyroidism, valvular heart disease, heart failure of New York Heart Association class III or IV, a left ventricular ejection fraction ≤40%, a LA diameter exceeding 50 mm, an LA thrombus, documented carotid stenosis, previous ischemic stroke or transient ischemic attacks, prior cardiac surgery or ablation in the LA, unstable angina or myocardial infarction within the last 3 months, severe chronic obstructive pulmonary disease, known bleeding disorders, and contraindication to oral anticoagulation and pregnancy. The study was approved by the local ethics committee.

After inclusion, patients were randomized into 3 different treatment groups: PVI with a CB catheter and the intraoperative administration of heparin to reach a minimum activated clotting time (ACT) level of 250 s according to the Venice Chart Consensus Protocol on Atrial Fibrillation Ablation[11] (CRYO group); PVI with the PVAC and also the conventional intraoperative anticoagulation protocol (ACT>250 s; PVAC group); and PVI performed with the PVAC using an anticoagulation protocol with an ACT target of >320 s (PVAC high-ACT group).

Patient Preparation and Ablation Procedure

Patients were hospitalized 1 or 2 days before the procedure. In patients taking oral anticoagulation, the drug was continued and the procedure was performed with an international normalized ratio in the therapeutic range. In all other patients, low–molecular-weight heparin was started twice daily in a weight-adjusted dose and administered until 12 hours before the procedure. Transesophageal echocardiography was carried out within 24 hours before the procedure to rule out the presence of a cardiac thrombus.

All procedures were performed under conscious sedation, using midazolam and fentanyl. Decapolar and quadripolar catheters were advanced from the femoral vein and positioned in the coronary sinus and the right ventricle. A single transseptal puncture was performed under fluoroscopic and ICE guidance, using a standard technique. A deflectable 12-Fr long sheath (FlexCath, Medtronic CryoCath LP, Kirkland, Quebec, Canada) was used in the LA and flushed continuously with heparinized saline at a steady rate of 30 mL/h throughout the procedure to minimize microbubble generation on ICE. This sheath was used as a guide with either the PVAC or the CB catheter. Immediately after transseptal puncture, a 150-IU/kg body weight intravenous heparin bolus was given, followed by a continuous infusion to maintain the predefined minimum target ACT level (250 or 320 s). ACT was always checked before the first ablation and every 20 minutes thereafter. Additional 2000- to 5000-IU IV boluses of heparin were administered, if needed, to reach the minimum target ACT level.

The technology of CB ablation has been described in detail.[12] A 28-mm balloon was used exclusively in all cases. The balloon was introduced into the PV ostium over the Achieve guidewire (Medtronic Ablation Frontiers, LLC, Carlsbad, CA), which is capable of mapping PV potentials before, during, and after cryo applications. Occlusion of the vein was assessed by means of a hand-held injection of contrast medium through the Arctic Front catheter. A minimum of two 5-minute freezing cycles were applied per PV. PVI was assessed on the basis of signals recorded by the Achieve wire.

The technical specifications of the PVAC and the GENius RF generator (Medtronic Inc, Minneapolis, MN) have been described in detail.[13–15] The catheter was advanced through the FlexCath sheath over a 0.032-inch guidewire, which was positioned selectively in each PV. The positions of the electrodes relative to the PV ostium were always confirmed before the first RF delivery, by means of selective contrast injection through the FlexCath sheath. The PVAC was connected to the GENius RF generator, which is capable of delivering RF current in different bipolar/unipolar mode ratios to any or all of the 5 bipolar channels in a duty-cycled mode. The target temperature was 60°C, measured separately for all bipoles. Bipolar/unipolar RF delivery was started at a ratio of 4:1 for each PV and changed to a bipolar/unipolar proportion of 2:1 or 1:1 for a deeper lesion when a sufficient reduction in local electrogram amplitude could not be achieved after multiple RF deliveries. RF energy was applied for 60 s, at least 3 to 4 times per PV. RF was delivered to all poles during initial applications at each PV. Later, usually after multiple energy deliveries, electrode pairs were selected on the bases of local electrograms. Importantly, any electrode pair that failed to reach ≥50°C during RF delivery was switched off to avoid ineffective energy delivery and thrombus formation because of improper contact at the electrode–tissue interface. Furthermore, when any electrode reached the target temperature while delivering very low power (1–2 W), it was considered a sign of an undesirably strong electrode–tissue contact or a wedge position of the electrode, and energy delivery to that particular electrode was switched off. The end point was electric isolation of all PVs, as confirmed by demonstrating an entrance block.

TCD Recording and Evaluation

TCD recording was performed throughout the whole period of LA access. The transducer was held in place by a proprietary headpiece supplied with the system. The middle cerebral arteries were bilaterally insonated from transtemporal windows by using a multifrequency Doppler (Multi Dop T digital, DWL, QL software version 2.8), which insonates simultaneously with 2- and 2.5-MHz frequencies. The system is capable of the automatic online identification of true MESs with a sensitivity of 100% and a specificity of 99.3%,[16] and also of

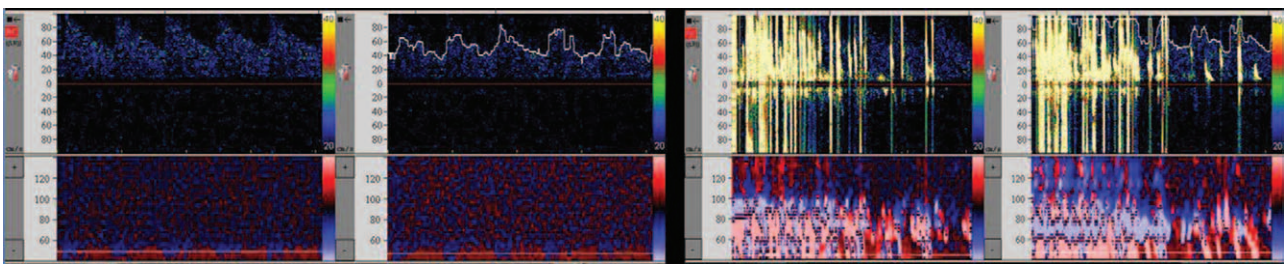

Figure 1. Bilateral multifrequency transcranial Doppler monitoring of middle cerebral arteries. Representative transcranial Doppler picture showing a baseline curve (left) and a burst of microembolic signals (right; high-intensity transient signals) during pulmonary vein angiography.

Figure 2. Assessment of microbubble formation on intracardiac echocardiography.

discrimination between gaseous and solid emboli with a specificity of 96.5%.[17] The identification of true MESs with parallel artifact rejection is possible by implementing an event detector system, using a previously published algorithm to detect high-intensity signals because of emboli.[16] This step is followed by a second algorithm using data from the dual-frequency insonation to determine whether the MESs are attributed to a solid or to a gaseous embolus. Differentiation is possible because the reflection of ultrasound power is dependent not only on the size of the embolus, but also on its composition and the insonating frequency used: solid emboli reflect more ultrasound at 2 MHz than at 2.5 MHz, whereas the opposite is true for gaseous emboli.

TCD parameter settings as recommended by the consensus criteria[18] were kept constant during the procedures. The insonation depth was 45 to 55 mm, the sample volume was 8 mm, and the power was 60 to 100 mW. An example of a TCD record is given in Figure 1.

MES counts were collected and evaluated separately during different stages of the procedure as follows:

1. Transseptal puncture: the 30-s period after crossing the interatrial septum with the transseptal needle.
2. PV angiography: contrast injection through the injection port of the CryoCath catheter or the transseptal sheath during PVAC ablation.
3. Energy delivery: from the start to 15 s after the termination of energy delivery.
4. The remainder of the procedure: that part of the LA access period during which none of the aforementioned maneuvers were performed.

ICE Monitoring

During each ablation phase, ICE was used for a semiquantitative characterization of the bubble formation by grouping them into 3 categories based on the bubble density.[9] Isolated bubbles were categorized as "few," those with a continuous but not dense appearance as "moderate," and those with a continuous and dense appearance as "shower" (Figure 2).

Statistical Methods

Data were derived by summing signal counts during the entire intervention, and also for the categories of each investigated factor defined by the ablation stage, whether electrodes 1 and 5 were simultaneously operating, and the bipolar-to-unipolar energy ratio. Gaseous and solid signal counts were summed (total signal count). Variables for signal count data were natural log-transformed to improve normality. Multilevel mixed-effects linear regression was used to evaluate the effects of the ablation type and the investigated factors (procedure stage, electrode 1+5 simultaneous operation, bipolar/unipolar ratio) on the total signal count. The number of models and the number of investigated factors fitted were the same, with interaction terms between the ablation type and the factor in each. The models were also adjusted for further variables found to be useful additions because of the consequential improvement of the model fit or the elimination of confounding. Fixed effects were expressed as estimated differences in the log-transformed outcome, 95% confidence intervals, and *P* values. Model checking was based on inspection of the normality of residuals. *P* values <0.05 were interpreted as indicating statistical significance.

For unadjusted descriptive tables of patient clinical characteristics and procedural data, Fisher exact test was used to compare the 3 groups in terms of categorical variables: for continuous variables, appearing in these tables, and in the descriptive figure for total signal count, the assumptions regarding normality (D'Agostino test) and homoscedasticity (Levene robust test) were checked and analysis of variance was used if both were satisfied; otherwise, the Kruskall–Wallis test was applied.

We carried out post hoc power calculations based on sample sizes, means, and SDs of the primary outcome variable (total signal count)

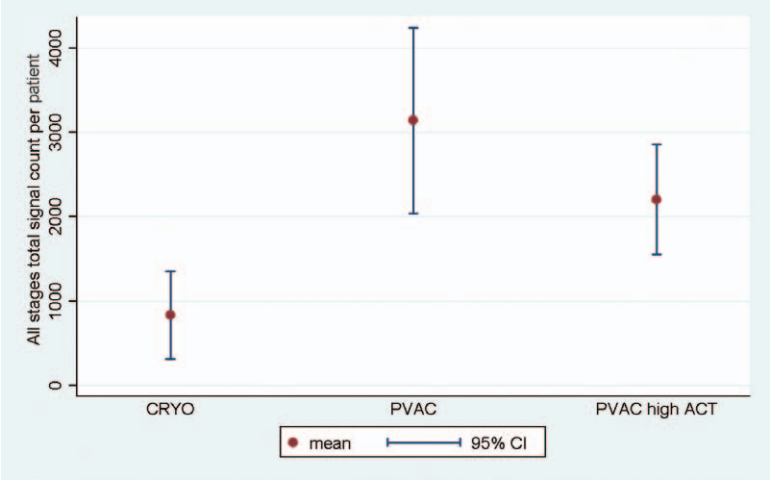

Figure 3. Total microembolic signal count in the 3 treatment groups. Graph depicting mean number of microembolic signals (MESs) per patient in each treatment group. ACT indicates activated clotting time; CI, confidence interval; and PVAC, pulmonary vein ablation catheter.

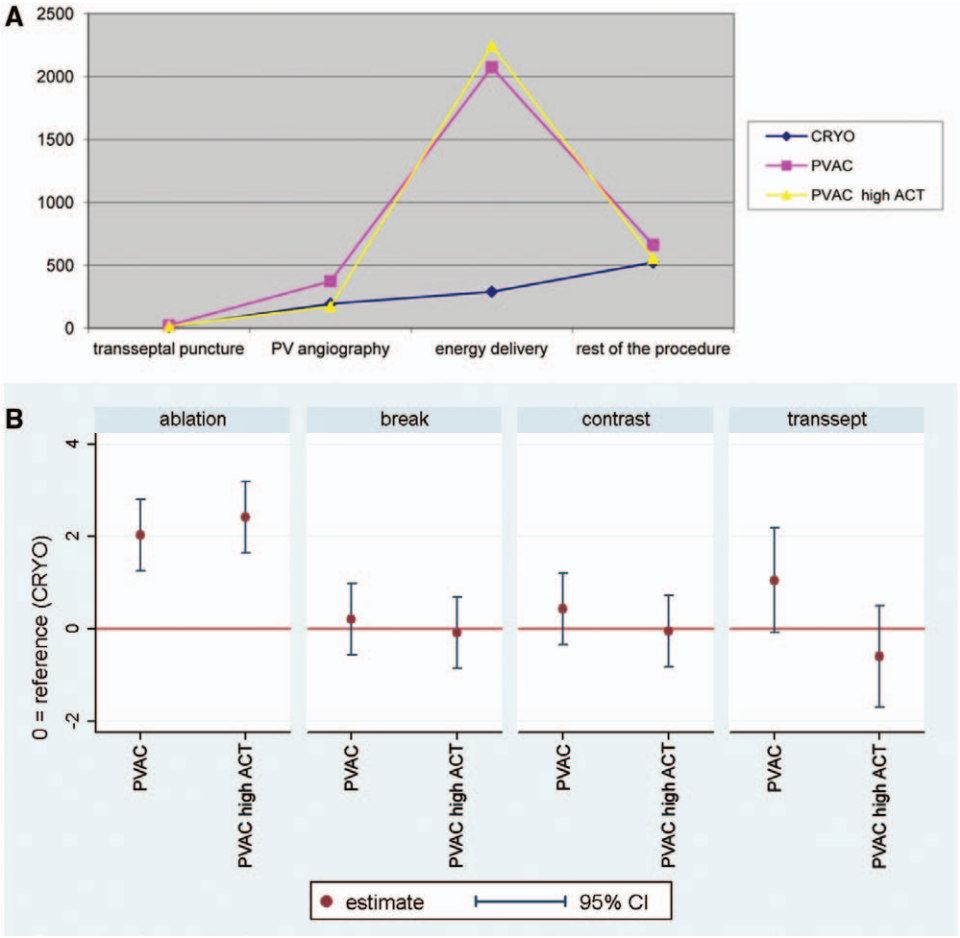

Figure 4. Microembolic signal count during different stages of the procedure. **A**, Trend of microembolus formation during different stages of the procedure, showing a peak of embolus generation during energy delivery in the case of pulmonary vein ablation catheter (PVAC), whereas no peak is seen during cryoballoon procedures. **B**, Comparison of microembolic signal (MES) counts during different stages of the procedure in the 3 treatment groups. As regards the MES count during cryoablation as a reference, a statistically significant difference between the 3 treatment groups is seen only in the case of the energy-delivery period. ACT indicates activated clotting time; and CI, confidence interval.

observed in all possible pairings of groups of the investigated factors, after the 2-sample comparison of means scenario (taking sample independence or paired nature into account), 2-sided test, α=0.05. Data were reduced to a single-record-per-subject structure by averaging or exclusion. We obtained for the detection of between-groups differences in relation to ablation type across all stages (power >0.9 in 2 of 3 possible pairings), ablation type in the ablation stage (power >0.9 in 2 of 3 pairings), bipolar/unipolar ratio (power >0.9 in 1 of 4 pairings, stratification for ablation type), electrode 1+5 simultaneous operation (power >0.9 in 1 of 2 pairings, same stratification), and procedure stage (power >0.9 in 11 of 18 pairings, same stratification); power figures for selected group pairings were <0.9, ranging from 0.05 to 0.89 (power >0.8 in 4 of 13 such pairings).

The statistical package Stata (Stata Corp. 2009, Statistical Software: Release 11, College Station, TX: Stata Corp LP) was used for statistical analysis.

Results

Patient Characteristics

A total of 34 patients who participated in 35 procedures were enrolled in this study. Table 1 presents clinical parameters of the patients in the 3 treatment groups. There were no significant differences in the baseline characteristics.

Table 1. Patient Clinical Characteristics

Demographic Variable	CRYO	PVAC	PVAC High ACT	*P* Value
N	10	12	13	
Age, y (SD)	54.3 (16.3)	47.5 (14.1)	53.6 (9.8)	0.4
Sex (male:female)	8:2	8:4	10:3	0.7
Paroxysmal:persistent AF, n	8:2	8:4	9:4	0.8
$CHADS_2$ score (SD)	0.5 (0.7)	0.6 (0.7)	0.8 (0.9)	1.0
LVEF, % (SD)	55.8 (4.2)	55.1 (9.1)	54.3 (6.2)	0.9
LAD, cm (SD)	41.9 (4.3)	39.9 (4.2)	41 (4.1)	0.5
Aspirin, n	2	3	6	0.3
Preprocedure therapeutic INR, n	2	2	6	0.1

AF indicates atrial fibrillation; INR, international normalized ratio; LAD, left atrial diameter; LVEF, left ventricular ejection fraction; and PVAC, pulmonary vein ablation catheter.

Procedural Data

Procedural data are listed in Table 2. The total procedure time, the total fluoro time, and the total energy delivery time were significantly longer in the CRYO group than in the PVAC groups. The mean ACT values also differed significantly in the 3 treatment groups according to the predefined protocol. No procedure-related complication was encountered in any patient.

MES Count

Because bilateral insonation of the middle cerebral arteries could not be achieved in all patients for technical reasons, MES counts were based on TCD recording of 16,22, and 23 arteries in the CRYO, PVAC, and PVAC high-ACT treatment groups, respectively. Mean MES counts per patient were calculated using either the mean of the bilateral counts when both sides were measured, or the unilateral data when only 1 side was available. As shown in Figure 3, cerebral MES count was significantly lower in the CRYO group as compared with the 2 PVAC groups (P=0.0005). No statistical difference was found between the 2 PVAC groups at this sample size (P=0.1419).

As regards the MES count during the different stages of the procedure, a relatively even distribution of embolus formation was found across the whole LA access time with CB, whereas the embolus formation was concentrated in the energy-delivery period with PVAC (Figure 4, top). The statistically significant difference seen in the total MES count could therefore be attributed to the difference during energy delivery (Figure 4, bottom).

The ratios of gaseous versus solid MESs detected in the 3 treatment groups are illustrated in Figure 5. Less than 20% of all microemboli were categorized as solid in all 3 groups. This ratio was constant across the different stages of the procedure.

Two ablation parameters potentially influencing the MES counts during the PVAC procedures were also analyzed: RF delivery with different bipolar/unipolar ratios, and the use versus the avoidance of simultaneous energy delivery on PVAC pairs 1 and 5. The latter was a significant predictor for a higher MES count in the normal-ACT PVAC group (P=0.036), but the bipolar/unipolar ratio did not influence MES formation.

Correlation Between ICE and MES Count

A significant correlation was found between bubble formation on ICE and the generation of MESs in all 3 groups during the procedure (P<0.001). The average number of MESs/min corresponding to the different grades of bubble formation on the semiquantitative ICE scale is indicated in Figure 6. Bubble formation on ICE required a critical amount of MESs and was not sensitive to detect infrequent microembolization.

Miscellaneous Observations

A shower of bubbles on ICE mostly appeared 5 to 10 s after RF delivery had been started. The onset of the shower of bubbles was followed by bursts of MESs, usually 5 to 10 s later (Video in the online-only Data Supplement). The gradual decrease and disappearance of the MESs and bubbles was usually observed within 10 to 15 s after the termination of energy delivery (Video in the online-only Data Supplement). Catheter manipulation, especially rotation, during this period often resulted in a new burst of microemboli detected by both techniques. Switching off poles that did not reach the target temperature during RF delivery did not result in an apparent change in the degree of microembolus generation. However, in those rare instances when PVAC electrodes were dislodged from the ostium deeper into the PV, a rapid rise in temperature with low delivered power (1–2 W) was usually observed, indicating an excellent contact or a poor cooling effect from the blood. An abrupt and very marked microembolization was also observed in the majority of these cases, prompting an immediate termination of RF delivery. During CB procedures, a burst of MESs was usually observed after the balloon had deflated after the application.

Discussion

The clinical significance of silent cerebral lesions demonstrated by diffusion-weighted MRI studies[2–8] is currently unknown. Recent data indicate that the majority of them are only transient phenomena with a clear tendency to resolve within a few weeks, especially those with small diameters.[19] A potential relationship between subclinical cerebral ischemia and a longer-term deterioration in cognitive function has to be considered, although in 1 study a subtle cognitive impairment did not correlate with the appearance of new MRI lesions.[3]

Although cerebral MRI studies were of utmost importance in drawing attention to the entity of subclinical cerebral ischemia, its recognition after ablation is too late for the individual patient. The real-time monitoring of embolic traffic in the brain might be a useful approach if backed up by more clinical data. Kilicaslan et al[9] first reported on the MES count detected by TCD during point-by-point pulmonary antrum isolation with the use of nonirrigated RF catheters. They demonstrated that cerebral microembolization occurs during

Table 2. Procedural Characteristics of Population Divided Into Three Treatment Groups

Procedural Parameters	CRYO	PVAC	PVAC High ACT	P Value
Total procedure time, min (SD)	129.5 (23)	112.6 (11)	101.2 (21)	0.01
Fluoroscopy time, min (SD)	27.9 (8)	21.2 (5.6)	20 (7.9)	0.04
Total energy-delivery time, min (SD)	48 (7.07)	18.3 (7.5)	17.9 (2.1)	0.001
Mean ACT, s (SD)	284.7 (62)	261 (28)	374.4 (54)	0.0001
Time to transseptal puncture, min (SD)	43.3 (11.9)	41.5(10.6)	38.8 (13.8)	0.6
Acute success rate (% of isolated PV)	87	100	98	0.8

ACT indicates activated clotting time; and PVAC, pulmonary vein ablation catheter.

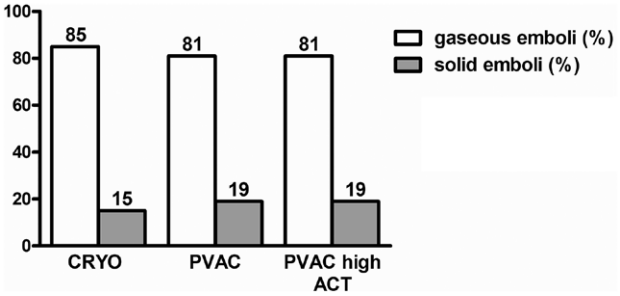

Figure 5. Ratio of gaseous/solid emboli in the 3 treatment groups. ACT indicates activated clotting time; and PVAC, pulmonary vein ablation catheter.

all PVI procedures. Moreover, an unexpectedly high number of cerebral microemboli was found as compared with those seen during cardiac surgery. Additionally, a significant correlation was demonstrated between the occurrence of manifest stroke and the number of MESs detected during the ablation procedure. Importantly, that study also proved the correlation between the MES count and the degree of microbubble formation on ICE. Similar data regarding the potential clinical significance of MES generation during CB ablation have not been published. Two other studies reported on cerebral microembolization detected by TCD during different AF ablation approaches recently.[10,20] In concordance with the MRI data, the number of MESs in these studies was dependent on the ablation technology.

This is the first study to our knowledge, which has also provided data regarding the composition of these microemboli by demonstrating that the majority of them are gaseous, solid particles occurring in <20% of them, regardless of the technology and the anticoagulation scheme used. Although not supported by scientific evidence, it is a general belief that gaseous emboli are less harmful than solid particles.[21] However, with similar proportions of solid MESs in the 3 treatment groups, the absolute number is significantly higher during PVAC ablation. Although none of our patients sustained a clinical stroke or transient ischemic attacks, longitudinal assessment of the cognitive function seems justified in these patients.

We found significant differences between CB and PVAC ablation in the temporal distribution of microembolus formation throughout the whole LA access time. The even distribution with CB technology suggests that catheter manipulation, inflation, and deflation of the balloon, and contrast injections into PVs are mainly responsible for MES generation. In contrast, the majority of MESs during PVAC ablation were recorded at the time of energy delivery: microemboli usually appeared in large quantities 10 to 15 s after RF delivery had been started. Although RF delivery with different bipolar/unipolar ratios did not influence MES formation, simultaneous RF delivery on PVAC pairs 1 and 5 was a significant predictor for a higher MES count in the normal-ACT PVAC group. The likely explanation for this finding is a reduced interelectrode distance or electrode overlap because of anatomic constraint of the PVAC loop arguing for a careful assessment on fluoroscopy or even routine avoidance of simultaneous RF delivery on poles 1 and 10.

Similar to our findings, a significant correlation was reported between the quantity of MESs and the degree of bubble formation detected by ICE,[9] the latter being used as a guide for power titration. An important difference between point-by-point RF and PVAC ablation, however, is that the power cannot be adjusted with the GENius ablator; indeed, the power management is entirely automatic, with no opportunity for the operator to exert control. Similar data regarding the potential clinical significance of MES generation during CB ablation have not been published.

Several hypotheses have been put forward to explain the potential mechanism of thrombus formation with the PVAC catheter. Because PV ostia and antra are widely variable in size and shape, a good tissue contact simultaneously with all electrodes of the circular PVAC that comes only in 1 size and shape may not always be possible. Increased char formation on noncontact electrode tips and dislodgment of thrombi from the endothelium acutely damaged by RF applications during subsequent catheter rotations is a plausible explanation, which was supported by our observation that especially shortly after the termination of RF delivery, catheter manipulations often resulted in the reinitiation of MES formation. Another

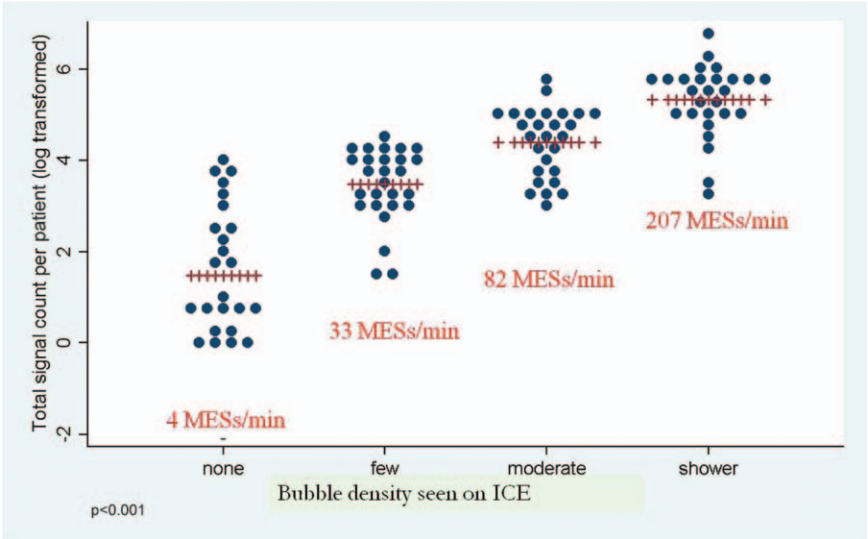

Figure 6. Correlation between degree of microbubble formation on intracardiac echocardiography (ICE) and the number of microembolic signals (MESs) detected by transcranial Doppler.

potential source of MES generation is tissue overheating. Tissue temperatures exceeding 80°C have been demonstrated to cause endothelial cell disruption, with the consequent loss of anticoagulation properties and heat-related denaturation of fibrinogen to fibrin, which in general might be responsible for a higher thrombogenicity of RF energy.[22–25] Irrigated RF catheters have been introduced into clinical practice to reduce thrombus formation through irrigation of the ablation electrode and reduction of the electrode–endothelium interface temperature. The original concept of the PVAC catheter and the GENius ablator was that the "off" phase of RF delivery with the duty-cycled mode provided enough time for the electrodes to cool down without using irrigation, thereby preventing thrombus formation on the electrodes. However, there are as yet no definitive data on whether duty-cycled RF energy with cooling by local blood flow provides the same protection from heating-related coagulum generation as open-irrigation catheters do. The MRI studies and our findings on the MES count do not seem to validate this concept.

The use of different ACT targets for intraprocedural heparinization did not result in a statistically significant impact on the MES count in this relatively small group of patients. The potential benefit of a more aggressive anticoagulation protocol needs to be assessed in larger-scale studies, although its impact on the mostly gaseous microemboli is questionable.

Currently available recommendations for periprocedural anticoagulation during AF ablation[11] may not apply uniformly to different ablation technologies involving the use of different types of energy. Instead, procedure-specific protocols need to be elaborated to maximize patient safety.

Limitations

The sample size in this study was relatively small. Nevertheless, a marked statistical difference was found between the CB and PVAC technologies in the number of cerebral MESs. However, the roles of different intraprocedural anticoagulation regimes need to be investigated in larger patient cohorts.

Our study compared 2 single-shot technologies assumed to have the least and the most thromboembolic potential based on previous cerebral MRI data. Including open-irrigated RF ablation as the most commonly used technology seems to be also important for future comparison.

The detection of silent cerebral lesions by diffusion-weighted-MRI was not included in our study because available data were consistent regarding their incidence with these ablation technologies. However, simultaneous assessment of MESs detected in the middle cerebral artery and silent lesions depicted by diffusion-weighted-MRI in other territories of the brain might have provided additional and complementary information.

We examined cerebral MES as a surrogate marker of the risk of neurological complications and did not include a clinical evaluation of the potential deleterious consequences of MESs. Assessment of subtle changes in cognitive function by comparing preoperative and postablation results should be an important aspect in future studies.

Bilateral TCD recording was not possible in a minority of our patients because of technical reasons; therefore, MES counts were reported as a mean per patient. Therefore, data from patients with MES detection on 1 side have half the weight compared with those with bilateral detection. This could have potentially led to a confounding variable affecting the analysis. However, previous studies in agreement with our interim analysis have consistently shown no side differences in the number of MESs recorded by TCD.

Differentiation between solid versus gaseous microemboli was automatic. In the validation studies[16,17] of this TCD system, gaseous and solid MESs were differentiated with 96% specificity. Furthermore, in a feasibility study performed in 10 patients with a different TCD equipment and manual counting of MESs we found a solid/gaseous microemboli ratio of 19/81, in agreement with the results obtained with automatic differentiation.

Conclusions

Cerebral microembolization was assessed by using TCD to compare AF ablation with a CB catheter versus PVAC and phased RF. In line with the results of previous MRI studies on the incidence of silent cerebral lesions, phased RF ablation was associated with significantly more MESs than CB ablation. Use of higher ACT target for intraoperative heparinization during PVAC ablation resulted in a trend to a lower MES count that did not reach statistical significance at the size of our patient cohort. Although the occurrence of MESs exhibited an even distribution during CB ablation, it was concentrated during RF delivery with phased RF technology. The majority of MESs were gaseous, regardless of the ablation technique and the phase of the procedure.

Disclosures

None.

References

1. Kok LC, Mangrum JM, Haines DE, Mounsey JP. Cerebrovascular complication associated with pulmonary vein ablation. *J Cardiovasc Electrophysiol*. 2002;13:764–767.
2. Schrickel JW, Lickfett L, Lewalter T, Mittman-Braun E, Selbach S, Strach K, Nähle CP, Schwab JO, Linhart M, Andrié R, Nickenig G, Sommer T. Incidence and predictors of silent cerebral embolism during pulmonary vein catheter ablation for atrial fibrillation. *Europace*. 2010;12:52–57.
3. Schwarz N, Kuniss M, Nedelmann M, Kaps M, Bachmann G, Neumann T, Pitschner HF, Gerriets T. Neuropsychological decline after catheter ablation of atrial fibrillation. *Heart Rhythm*. 2010;7:1761–1767.
4. Gaita F, Caponi D, Pianelli M, Scaglione M, Toso E, Cesarani F, Boffano C, Gandini G, Valentini MC, De Ponti R, Halimi F, Leclercq JF. Radiofrequency catheter ablation of atrial fibrillation: a cause of silent thromboembolism? Magnetic resonance imaging assessment of cerebral thromboembolism in patients undergoing ablation of atrial fibrillation. *Circulation*. 2010;122:1667–1673.
5. Neumann T, Kuniss M, Conradi G, Janin S, Berkowitsch A, Wojcik M, Rixe J, Erkapic D, Zaltsberg S, Rolf A, Bachmann G, Dill T, Hamm CW, Pitschner HF. MEDAFI-Trial (Micro-embolization during ablation of atrial fibrillation): comparison of pulmonary vein isolation using cryoballoon technique vs. radiofrequency energy. *Europace*. 2011;13:37–44.
6. Lickfett L, Hackenbroch M, Lewalter T, Selbach S, Schwab JO, Yang A, Balta O, Schrickel J, Bitzen A, Lüderitz B, Sommer T. Cerebral diffusion-weighted magnetic resonance imaging: a tool to monitor the thrombogenicity of left atrial catheter ablation. *J Cardiovasc Electrophysiol*. 2006;17:1–7.
7. Herrera Siklódy C, Deneke T, Hocini M, Lehrmann H, Shin DI, Miyazaki S, Henschke S, Kalusche D, Haissagure M, Arentz T. Incidence of asymptomatic intracranial embolic events after pulmonary vein isolation. Comparison of different atrial fibrillation ablation technologies in a multicenter study. *J Am Coll Cardiol*. 2011;58:681–688.

8. Gaita F, Leclercq JF, Schumacher B, Scaglione M, Toso E, Halimi F, Schade A, Froehner S, Ziegler V, Sergi D, Cesarani F, Blandino A. Incidence of silent cerebral thromboembolic lesions after atrial fibrillation ablation may change according to technology used: comparison of irrigated radiofrequency, multipolar nonirrigated catheter and cryoballoon. *J Cardiovasc Electrophysiol*. 2011;22:961–968.
9. Kilicaslan F, Verma A, Saad E, Rossillo A, Davis DA, Prasad SK, Wazni O, Marrouche NF, Raber LN, Cummings JE, Beheiry S, Hao S, Burkhardt JD, Saliba W, Schweikert RA, Martin DO, Natale A. Transcranial Doppler detection of microembolic signals during pulmonary vein antrum isolation: implications for titration of radiofrequency energy. *J Cardiovasc Electrophysiol*. 2006;17:495–501.
10. Sauren LD, Van Belle Y, De Roy L, Pison L, LA Meir M, Van der Veen FH, Crijns HJ, Jordaens L, Mess WH, Maessen JG. Transcranial measurement of cerebral microembolic signals during endocardial pulmonary vein isolation: comparison of three different ablation techniques. *J Cardiovasc Electrophysiol*. 2009;20:1102–1107.
11. Natale A, Raviele A, Arentz T, Calkins H, Chen SA, Haïssaguerre M, Hindricks G, Ho Y, Kuck KH, Marchlinski F, Napolitano C, Packer D, Pappone C, Prystowsky EN, Schilling R, Shah D, Themistoclakis S, Verma A. Venice Chart international consensus document on atrial fibrillation ablation. *J Cardiovasc Electrophysiol*. 2007;18:560–580.
12. Van Belle Y, Janse P, Rivero-Ayerza MJ, Thornton AS, Jessurun ER, Theuns D, Jordaens L. Pulmonary vein isolation using an occluding cryoballoon for circumferential ablation: feasibility, complications, and short-term outcome. *Eur Heart J*. 2007;28:2231–2237.
13. Boersma LV, Wijffels MC, Oral H, Wever EF, Morady F. Pulmonary vein isolation by duty-cycled bipolar and unipolar radiofrequency energy with a multielectrode ablation catheter. *Heart Rhythm*. 2008;5:1635–1642.
14. Scharf C, Boersma L, Davies W, Kanagaratnam P, Peters NS, Paul W, Rowland E, Grace A, Fynn S, Dang L, Oral H, Morady F. Ablation of persistent atrial fibrillation using multielectrode catheters and duty-cycled radiofrequency energy. *J Cardiovasc Electrophysiol*. 2010;21:399–405.
15. Boersama L, Duytschaever M, Geller JC, Scarf C. *The PVAC Workbook*. London, UK: Remedica; 2010:1–21, 41–67.
16. Russell D, Brucher R. Online automatic discrimination between solid and gaseous cerebral microemboli with the first multifrequency transcranial Doppler. *Stroke*. 2002;33:1975–1980.
17. Markus HS, Punter M. Can transcranial Doppler discriminate between solid and gaseous microemboli? Assessment of a dual-frequency transducer system. *Stroke*. 2005;36:1731–1734.
18. Ringelstein EB, Droste DW, Babikian VL, Evans DH, Grosset DG, Kaps M, Markus HS, Russell D, Siebler M. Consensus on microembolus detection by TCD. International Consensus Group on Microembolus Detection. *Stroke*. 1998;29:725–729.
19. Deneke T, Shin DI, Balta O, Bünz K, Fassbender F, Mügge A, Anders H, Horlitz M, Päsler M, Karthikapallil S, Arentz T, Beyer D, Bansmann M. Postablation asymptomatic cerebral lesions: long-term follow-up using magnetic resonance imaging. *Heart Rhythm*. 2011;8:1705–1711.
20. Sauren LD, la Meir M, de Roy L, Pison L, van der Veen FH, Mess WH, Crijns HJ, Maessen JG. Increased number of cerebral emboli during percutaneous endocardial pulmonary vein isolation versus a thoracoscopic epicardial approach. *Eur J Cardiothorac Surg*. 2009;36:833–837.
21. Neville MJ, Butterworth J, James RL, Hammon JW, Stump DA. Similar neurobehavioral outcome after valve or coronary artery operations despite differing carotid embolic counts. *J Thorac Cardiovasc Surg*. 2001;121:125–136.
22. Khairy P, Chauvet P, Lehmann J, Lambert J, Macle L, Tanguay JF, Sirois MG, Santoianni D, Dubuc M. Lower incidence of thrombus formation with cryoenergy versus radiofrequency catheter ablation. *Circulation*. 2003;107:2045–2050.
23. Anfinsen OG, Gjesdal K, Brosstad F, Orning OM, Aass H, Kongsgaard E, Amlie JP. The activation of platelet function, coagulation, and fibrinolysis during radiofrequency catheter ablation in heparinized patients. *J Cardiovasc Electrophysiol*. 1999;10:503–512.
24. Haines D. Biophysics of ablation: application to technology. *J Cardiovasc Electrophysiol*. 2004;15(10 suppl):S2–S11.
25. Haines DE, Watson DD. Tissue heating during radiofrequency catheter ablation: a thermodynamic model and observations in isolated perfused and superfused canine right ventricular free wall. *Pacing Clin Electrophysiol*. 1989;12:962–976.

CLINICAL PERSPECTIVE

Fresh, clinically silent cerebral ischemic lesions after catheter ablation of atrial fibrillation have been recently demonstrated on diffusion MR with an incidence consistently related to the ablation technology. We compared intraoperative microembolization as assessed by the number of microembolic signals in the cerebral arteries detected by transcranial Doppler during pulmonary vein isolation with 2 techniques: cryoballoon and phased radiofrequency (RF) ablation. In line with the findings of previous MRI studies, we found significant difference in the total count of microembolic signals, which were almost double during phased RF as compared with cryoballoon ablations. An even distribution of microembolization was demonstrated throughout the procedure during cryoballoon ablation, whereas microembolization was related to energy delivery with the phased RF technique. Almost 80% of microemboli were gaseous in nature with both technologies, and a higher activated clotting time target during phased RF ablation failed to reduce microembolization significantly. Our data suggest that postablation cerebral lesions may represent a cumulative effect of microembolization during the ablation. More aggressive intraprocedural heparinization might be of limited or no value in reducing dominantly gaseous microemboli. Because the majority of microemboli are generated by energy delivery with phased RF, biophysical reengineering of the generator might be required for safer ablation.

SUPPLEMENTAL MATERIAL

Patient ID	Type of ablation	Age	Gender	Type of AF	CHADS2 score	LV EF (%)	LAD (cm)	Aspirin	Preprocedure INR
Patient 1	CRYO	72	female	paroxismal	2	62	43	no	<2
Patient 2	CRYO	63	male	paroxismal	1	56	40	no	<2
Patient 3	CRYO	23	male	persistent	0	54	42	no	<2
Patient 4	CRYO	64	female	paroxismal	0	50	33	no	<2
Patient 5	CRYO	51	male	paroxismal	0	57	48	no	2,83
Patient 6	CRYO	55	male	paroxismal	1	55	46	yes	<2
Patient 7	CRYO	51	male	paroxismal	1	52	38	no	2,11
Patient 8	CRYO	67	male	paroxismal	0	54	40	no	<2
Patient 9	CRYO	30	male	persistent	0	64	44	yes	<2
Patient 10	CRYO	67	male	paroxismal	0	54	45	no	<2
Patient 11	PVAC	55	male	paroxismal	2	33	49	yes	<2
Patient 12	PVAC	33	female	paroxismal	0	57	41	no	<2
Patient 13	PVAC	31	male	paroxismal	0	55	40	no	<2
Patient 14	PVAC	38	male	paroxismal	0	56	33	yes	<2
Patient 15	PVAC	55	male	persistent	0	56	38	no	<2
Patient 16	PVAC	51	male	paroxismal	1	52	38	no	2,66
Patient 17	PVAC	47	male	paroxismal	0	62	38	yes	<2
Patient 18	PVAC	69	female	paroxismal	2	60	40	no	2,38
Patient 19	PVAC	48	female	paroxismal	1	56	40	no	<2
Patient 20	PVAC	22	male	persistent	0	68	40	no	<2
Patient 21	PVAC	56	female	persistent	1	54	44	no	<2
Patient 22	PVAC	65	male	persistent	1	53	38	no	<2
Patient 23	PVAC high ACT	63	male	paroxismal	2	42	47	no	<2
Patient 24	PVAC high ACT	56	female	paroxismal	2	60	35	yes	2,76
Patient 25	PVAC high ACT	43	male	persistent	0	42	44	yes	2,02
Patient 26	PVAC high ACT	32	male	paroxismal	0	60	38	no	<2
Patient 27	PVAC high ACT	56	male	persistent	1	58	48	no	<2
Patient 28	PVAC high ACT	56	male	paroxismal	0	52	39	no	2,25
Patient 29	PVAC high ACT	56	male	paroxismal	0	59	38	yes	2,95
Patient 30	PVAC high ACT	58	male	persistent	1	54	44	no	<2
Patient 31	PVAC high ACT	49	male	persistent	0	50	38	yes	2,47
Patient 32	PVAC high ACT	68	male	paroxismal	3	56	42	no	<2
Patient 33	PVAC high ACT	63	female	paroxismal	1	57	39	yes	<2
Patient 34	PVAC high ACT	42	male	paroxismal	1	58	45	yes	2,29
Patient 35	PVAC high ACT	56	female	paroxismal	0	59	37	no	<2

Supplemental table 1. Individual patient information

Patient ID	Procedure Type	Total Procedure Time (min)	Fluoroscopy Time (min)	Total Energy Delivery Time (min)	Number of Energy Delivery	Mean ACT (s)	Procedure INR	Time to Transseptal Puncture (min)	Number of Switching Off Poles	PVAC Pairs 1,5 Simultaneously Active	Ratio of Gaseous Emboli	Ratio of Solid Emboli
Patient 1	CRYO	108	24,9	40	8	415	<2	39	cryo	cryo	79	21
Patient 2	CRYO	140	28,6	35	7	305	<2	60	cryo	cryo	88	12
Patient 3	CRYO	150	31	35	7	257	<2	58	cryo	cryo	83	17
Patient 4	CRYO	157	27,3	70	14	261	<2	37	cryo	cryo	87	13
Patient 5	CRYO	136	34,9	65	13	349	2,83	27	cryo	cryo	83	17
Patient 6	CRYO	111	22	45	9	239	<2	45	cryo	cryo	82	18
Patient 7	CRYO	165	47	80	16	301	2,11	60	cryo	cryo	89	11
Patient 8	CRYO	118	15,05	45	9	290	<2	35	cryo	cryo	87	13
Patient 9	CRYO	113	29,9	35	7	224	<2	35	cryo	cryo	86	14
Patient 10	CRYO	97	19,2	25	5	206	<2	37	cryo	cryo	82	18
Patient 11	PVAC	95	20,4	18	18	316	<2	45	12	10	79	21
Patient 12	PVAC	118	27,3	16	16	242	<2	33	16	0	88	12
Patient 13	PVAC	112	20,8	21	21	220	<2	37	21	12	81	19
Patient 14	PVAC	120	28,4	20	20	283	<2	20	16	14	64	36
Patient 15	PVAC	116	14,5	11	11	235	<2	50	7	6	85	15
Patient 16	PVAC	104	17,56	5	5	250	2,66	38	3	3	84	16
Patient 17	PVAC	102	19	24	24	287	<2	35	15	16	84	16
Patient 18	PVAC	99	12,49	14	14	280	2,38	49	13	1	79	21
Patient 19	PVAC	120	17,4	19	19	227	<2	60	5	15	82	18
Patient 20	PVAC	139	27,8	18	18	262	<2	40	18	13	85	15
Patient 21	PVAC	115	19,5	27	27	253	<2	38	17	16	88	12
Patient 22	PVAC	112	29,3	27	27	282	<2	53	27	15	88	12
Patient 23	PVAC high ACT	85	17	15	15	347	<2	29	5	12	85	15
Patient 24	PVAC high ACT	120	11,4	17	17	354	2,76	58	13	6	85	15
Patient 25	PVAC high ACT	97	14,5	23	23	365	2,02	27	19	6	86	14
Patient 26	PVAC high ACT	125	22	24	24	375	<2	43	18	10	86	14
Patient 27	PVAC high ACT	97	15	9	9	353	<2	63	4	6	82	18
Patient 28	PVAC high ACT	112	17,4	18	18	356	2,25	50	2	18	85	15
Patient 29	PVAC high ACT	105	19	9	9	376	2,95	45	9	6	81	19
Patient 30	PVAC high ACT	101	31,1	22	22	372	<2	37	22	12	68	32
Patient 31	PVAC high ACT	150	35,1	17	17	533	2,47	40	6	12	85	15
Patient 32	PVAC high ACT	84	20,4	20	20	359	<2	23	4	17	82	18
Patient 33	PVAC high ACT	70	15,9	21	21	376	<2	15	15	9	82	18
Patient 34	PVAC high ACT	80	9,8	17	17	325	2,29	30	15	5	83	17
Patient 35	PVAC high ACT	90	31,5	21	21	376	<2	45	21	15	86	14

Supplemental table 2. Individual procedural information

SUPPLEMENTAL MATERIAL LEGENDS

Supplemental table 1. Individual patient information

Supplement table 2. Individual procedural information

Supplemental video 1. ICE monitoring: A shower of bubbles on ICE appeared 5-10 s after RF delivery had been started. The onset of the shower of bubbles was followed by bursts of MESs, 5-10 s later.

Supplemental video 2. ICE monitoring: The gradual decrease and disappearance of the MESs and bubbles observed within 10-15 s after the termination of energy delivery